TURBULENCE AS SOUND SOURCE IN SUBSONIC JETS

Odenir de Almeida, odenir@mecanica.ufu.br
Aristeu da Silveira Neto, aristeus@mecanica.ufu.br
Federal University of Uberlândia – UFU, Brazil
João Roberto Barbosa, barbosa@ita.br
Technologic Institute of Aeronautics – ITA, Brazil

Rodney Harold Self, rhs@isvr.soton.ac.uk
Institute of Sound and Vibration Research – ISVR, United Kingdom

Abstract. *The purpose of this work is to provide a general overview about turbulence as sound source in subsonic jets. Such phenomenon has been studied in the last 50 years, since the pioneering work of Sir James Ligthill, looking towards means of predicting noise caused by the inherent turbulence nature of the jet. However, only a few aspects have been understood and mathematically solved so far. The main mechanisms of energy transfer inside the jet structures are still a key point in this theory as well as the effects of anisotropy in a subsonic turbulent jet. Herein, some numerical results are also presented as part of an ongoing research to improve the spectral predictions obtained by using Lighthill Acoustic Analogy. The anisotropy effect is investigated by doing numerical simulations of subsonic jets operating at different Mach numbers by using a Reynolds Stress Turbulence Modelling (RSTM). The numerical results provided insights about the relationship between the integral length scales (longitudinal versus transverse) and the ratio between the velocity fluctuations in the corresponding streamwise and spanwise directions, respectively.*

1. INTRODUCTION

The role of turbulence in sound generation has been considered by a number of authors: Lighthill (1952, 1954), Meechan and Ford (1958) and others.

In general a turbulent jet flow at very large Reynolds numbers may be divided into a mean motion, U , a large scale turbulent motion, u', and a small scale turbulent motion, u'', which is almost independent of the large scale motion. It is assumed that the small scale turbulent motion at this large Reynolds number is in almost universal equilibrium.

This assumption exposes the wide range of scales, both in space and in time, always present in a turbulent flow. It is considered that the large scales are typically determined by the geometry of the flow while the size of the smallest scales decreases with increasing Reynolds number. Each flow structure commonly called either vortex or eddy can be related to a scale of velocity, time and length. Figure 1 illustrates the transition to turbulence process in a single jet flow. Figure 1(a) is a schematic drawing of the flow structures presented in this process. Figure 1(b) shows a flow visualization of a real jet, where it is possible to identify qualitatively the wide range of scales presented in the flow field.

In Figure 1(a) the numbers represent respectively: (1) convergent nozzle; (2) potential core; (3) toroid of high vorticity concentration; (4) generation of bidimensional toroidal vortices; (5) pairing of annular vortices; (6) tridimensional oscillations over toroidal vortices; (7) degeneration in tridimensional turbulence and (8) reorganization of big scale turbulence, which is composed by multiple scales structure.

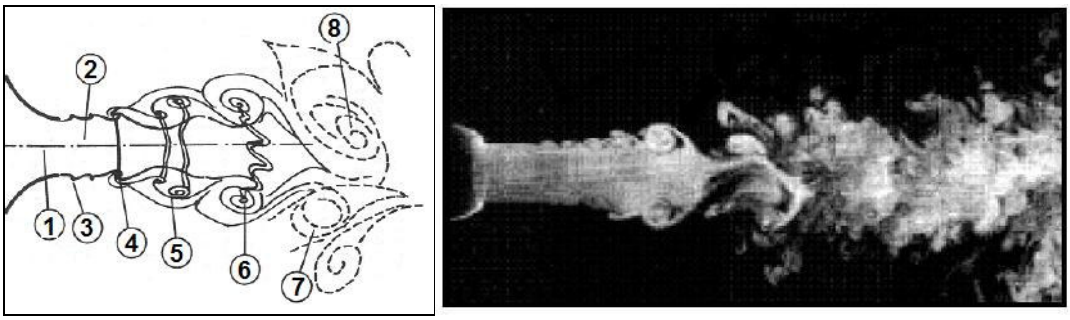

(a) Schematic Drawing (b) Flow Visualization

Figure 1. Illustration of the transition process in a single jet flow, after Silveira-Neto (2001).

Yule (1978), who carried out extensive visualization as well as conditional hot-wire measurements of these structures in moderate Reynolds number low-speed jets, suggested that the jet mixing layer be divided into two regions,

shown in Figure 1(a) as number 2 and 6. In the transitional-flow region (between 2 and 6) closest to the nozzle exit, the shear layer rolls up into toroidal vortices. These toroidal vortices are the equivalent of the large vortical structures of the two-dimensional mixing layer described above. The vortices undergo pairing and tearing. Further downstream in the turbulent flow region they break up into three-dimensional large turbulent structures. These structures, which are made up of rotational fluid, have highly irregular boundaries and bear no resemblance to the strongly axisymmetric toroidal vortices. The axial length of the transitional-flow region where toroidal vortices are found depends on the Reynolds number. This region shortens as Reynolds number increases. Thus, for high Reynolds number jets, vortex pairing is, in fact, an infrequent event. The pairing process, therefore, is not expected to be dynamically very significant for high Reynolds number jets.

2. TURBULENCE IN JET FLOWS

Beyond a qualitative description of the range of different scales structure in a jet flow, the turbulence theory defines three different length scales often related to a generic turbulent flow, which are: the integral length scale (l), the Taylor microscale (λ) and the Kolmogorov microscale (η).

The smallest length scales in a turbulent flow are the Kolmogorov microscales. It is generally accepted that the size of each of the turbulent length scales can be related to the energy spectrum – Figure 2 and moreover, that there is a cascade of energy from the largest to the smallest scales inherent to the turbulent flow. Detailed information about the energy distribution process in a turbulent flow can be found in textbooks as Tennekes and Lumley (1972) and Pope (2003). At this stage the important point is how the scales or structures inside the flow take part in the cascade process.

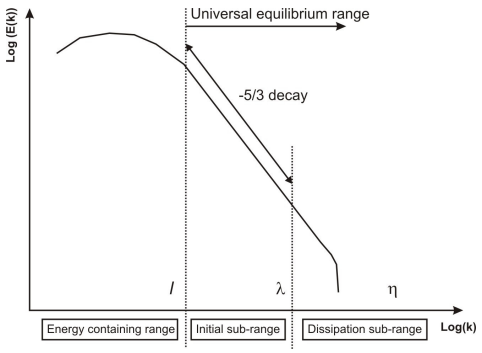

Figure 2. Turbulent kinetic energy spectrum.

The large scales contain most of the turbulent energy and transport the majority of the momentum and the energy which is continuously supplied by the mean flow. These larger eddies form what is known as the energy containing region and the length scales associated are the integral length scales, since they are determined mainly by the geometry of the flow. In the middle of the energy transfer process there is the inertial subrange, which is characterized by the Taylor length scale. As the name suggests, in this region the inertial forces begin to dominate. This region transfers the energy from the large scales to the smaller scales.

The smallest scales in the energy spectrum are in the dissipation region. At this level, within the flow the viscosity is important and the entire kinetic energy of the eddies is transferred into heat by viscous dissipation. The Kolmogorov microscales are characteristic of this region. These smallest scales are then responsible for dissipating the energy and are considered to be isotropic. The Kolmogorov scales η are extremely small. Their ratio to the scales of the largest eddies is defined by:

$$\frac{\eta}{L_0} \propto (\mathrm{Re}_{L_0})^{-3/4} \tag{1}$$

where L_0 is the size of the largest scales. As can be inferred from Equation (1), as the Reynolds number increases the smaller will be the size of the Kolmogorov scales. As an example, a turbulent jet flow issuing from a nozzle of diameter of 0.05 m at Reynolds number 1×10^6 will have scales inside the flow of order 1.5×10^{-6} m.

The time scale ratio in terms of the flow Reynolds number is given by:

$$\frac{\tau_\eta}{\tau_0} \propto (\mathrm{Re}_{L_0})^{-1/2} \tag{2}$$

where τ_η and τ_0 are the time scale associated with the smallest eddies (Kolmogorov) and the time scale associated with the largest eddies in the flow.

In addition, Kolmogorov microscales can be estimated presuming that the smallest eddies depend only on the rate at which the energy is transferred from the large structures and the viscosity. The smallest scales for length and time of a turbulent flow are given as function of the kinematic viscosity and the dissipation rate of turbulent kinetic energy as:

$$\eta = \left(\frac{\nu^3}{\varepsilon}\right)^{\frac{1}{4}} \tag{3}$$

$$\tau_\eta = \left(\frac{\nu}{\varepsilon}\right)^{\frac{1}{2}} \tag{4}$$

where η and τ_η are the Kolmogorov length and time scales, respectively.

The Kolmogorov and Taylor microscales can be related to the integral scales through the turbulent Reynolds number (Re_t) as presented in Table 1 below.

Table 1. Relationship among length and time scales in a turbulent flow.

	Length Scale	Time Scale
Kolmogorov	$\frac{\eta}{l} \propto (\mathrm{Re}_t)^{-\frac{3}{4}}$	$\frac{\tau_\eta}{t_l} \propto (\mathrm{Re}_t)^{-\frac{1}{2}}$
Taylor	$\frac{\lambda}{l} \propto (\mathrm{Re}_t)^{-\frac{1}{2}}$	$\frac{\tau_\lambda}{t_l} \propto (\mathrm{Re}_t)^{-\frac{1}{4}}$

Figure 3 summarizes the energy cascade process in a turbulent jet flow, as previously discussed, identifying the limits among the scales in the flow field.

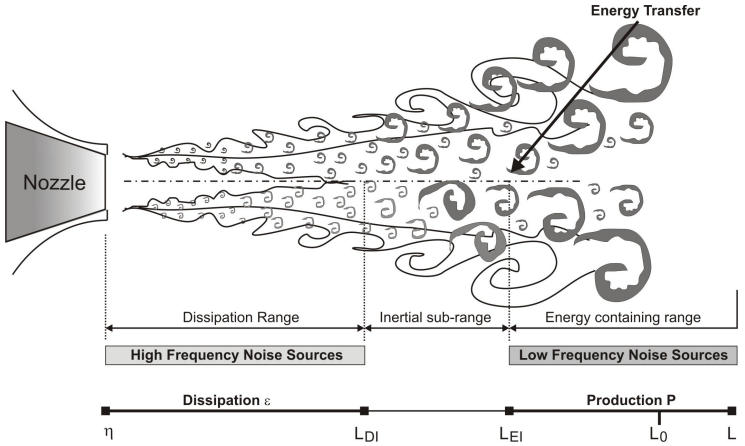

Figure 3. Energy cascade in a turbulent jet flow.

The limits between the different ranges can be roughly approximated using the following scales:

$$l_{DI} \approx 60\eta \tag{5}$$

$$l_{EI} \approx \frac{1}{6} L_0 \tag{6}$$

Having defined the length scales, the time scales associated with each portion of the flow will now be characterized. As summarized in the work of Azarpeyvand (2008), in general time scales of a jet flow can be:

- those related to the development of the whole flow;
- those associated with the interaction of the mean flow and the turbulence;
- and finally those that provide a measure of the action of the turbulence on itself.

These three scales can be alternatively described as the mean flow strain rate scale, the turbulence production scale, and the turbulence decay scale. The time scale associated with the first phenomenon, τ_s, gives an estimate of the rate of change of the mean velocity. The production time scale, τ_p, indicates the time needed to produce an amount of energy k at the rate of the production of turbulent kinetic energy ($\Pr$), and finally, the dissipation time-scale, τ_d, gives an estimate of the time to dissipate an amount of energy k at the constant rate ε. These time scales are then defined as:

$$\tau_d \propto \frac{k}{\varepsilon}, \qquad \tau_s \propto \left|\frac{dU}{dr}\right|^{-1}, \qquad \tau_p \propto \frac{k}{\Pr} \tag{7}$$

The dissipation and production time scales are roughly equal and are the largest time scales of the turbulence. The strain rate time scale, τ_s, gives an estimate of variation of the mean flow velocity in the radial direction, which is a measure of the evolution time of the largest eddies, and it is not, therefore, of great concern.

2.1. Theory on Sound of Jets

Once the role of the turbulent structures inside the flow has been defined, the next logical step in the development of the theory of sound production by turbulent jets would be the correlation of the flow dynamics with the noise production and propagation mechanisms. Therefore, before undertaking this task, a review of some of the relevant physical aspects of the jet noise theory will be given.

As a starting point, the general assumption that the noise of jets is caused by the strong and extremely turbulent mixing of the exhaust gases with the atmosphere is plausible. Moreover, the amount of noise generated is then influenced by the shearing action caused by the relative speed between the exhaust jet and the atmosphere. It is largely accepted that jet noise is related to:

- fine-scale fluctuations or turbulence;
- large scale coherent structures;
- screetch tones;
- and broadband shock-noise.

For supersonic jets only the last two mechanisms are dominant. In subsonic jets, the first mixing mechanism is expected to dominate except for certain cases of heated jets. As the sound generation mechanism is related to fine-scale fluctuations the jet noise spectrum measured from a subsonic jet has a broadband shape.

Figure 4 presents typical subsonic jet noise spectra at 90° observer position from the jet exhaust centerline for different discharge velocities. As can be seen, the nature of the spectrum is broadband without the presence of a very determined frequency peak.

It is important to emphasize that the large scale coherent structures are always present in a subsonic flow. These large scale structures seem to be a more effective noise contributor at moderate and low Reynolds number flows.

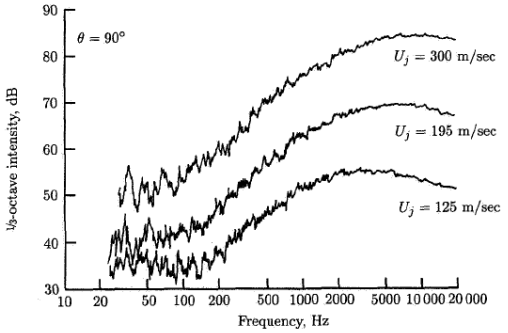

Figure 4. Subsonic jet noise spectra at 90° observer position, from Aeroacoustis of Flight Vehicles (1991).

In addition, as seen previously, when the exhaust jet velocity exceeds the local speed of sound, a regular shock pattern is formed within the exhaust jet core. This produces a discrete (single frequency) tone and selective amplification of the mixing noise, as shown in Figure 5. A reduction in noise level occurs if the mixing rate is accelerated or if the velocity of the exhaust jet relative to the atmosphere is reduced. This can be achieved by changing the pattern of the exhaust jet.

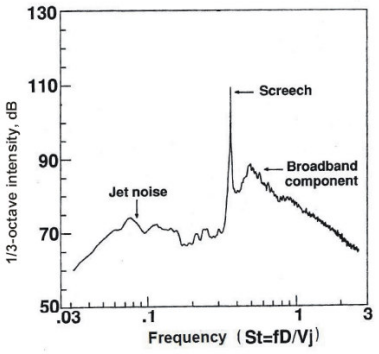

Figure 5. Shock associated spectra – Supersonic Jet Flow, from Aeroacoustis of Flight Vehicles (1991).

2.2. Fine and Large Scales (Eddies)

In growing shear layers, eddies are physically small near the origin of the shear layer. As the shear layer evolves downstream, eddies start to grow in size. However, at some axial location in the jet wake, both small and large scale eddies coexists. It is well known that the noise generated by these "small" or fine scales eddies will be of high frequency, while the "large" scale eddies downstream will be of lower frequency.

According to Meechan and Ford (1958) the bulk of the energy in the turbulent motion will reside in the large-scale eddies. Energy enters the turbulent cascade via the large eddies, so they control the overall amount of acoustic power. It is also well known that the number and size of these large eddies is dependent upon the manner in which the turbulence is produced. Since most of the acoustic radiation comes from the large-scale eddies, it is possible to say that the total acoustic power produced by a given turbulent motion will depend upon the manner in which the turbulence intensity is generated. Since the large-scale eddies produce the low-frequency sound, the low-frequency end of the power spectrum will depend upon the driving mechanism of the turbulence.

The high-frequency end of the spectrum, on the other hand, may be independent of the driving forces. This high-frequency sound is produced by the rapid fluctuations in the turbulent fluid. Moreover, the natural frequencies of the large-scale eddies are small, the rapid fluctuations being associated with the small-scale eddies. This is true despite the fact that the velocities associated with the large-scale eddies are greater. The small-scale eddies which give rise to the high-frequency components of the power spectrum may be thought of as being transported by the large-scale eddies, so that it is not possible to neglect the influence of the large-scale eddies on the high-frequency end of the power spectrum. This influence, however is, primarily a Doppler effect which may be neglected for low Mach number turbulence.

2.3. Self and Shear-Noise

The sound generated by a turbulent jet can be separated into two parts Ribner (1969). These contributions are:

- the sound generated by interaction of turbulence fluctuations and the sheared mean flow;
- and sound generated by turbulence fluctuations interacting with themselves;

The two sound components are often referred to as shear-noise and self-noise, respectively. For isotropic turbulence under no convection effects, the self noise is omni-directional, which means that it is radiated equally in all directions, whereas the shear noise gives a dipole-like contribution. Superimposed, these two contributions give an ellipsoid-shaped sound radiation pattern, with most sound radiated along the jet axis. Adding the effect of convection, the part of the sound that is radiated downstream of the jet is significantly larger than the part radiated in the upstream direction. Finally, the effect of refraction is to significantly decrease the sound radiated along the jet axis.

3. TURBULENCE AND THE NOISE PRODUCTION PROCESS

A turbulent jet flow can be split into three different turbulence regions: the dissipation range close to the jet nozzle, the inertial sub-range and the energy containing sub-range far downstream in the jet's wake. As part of the process of noise prediction is necessary to understand which of these regions are most contributing to the noise generation.

There are indications that the inertial subrange plays the most important role in the noise production mechanisms, Meechan and Ford (1958) and Rubinstein and Zhou (2000). It is important to remind that the inertial subrange acts like a connection between the energy containing range and the dissipation range, transferring the turbulent kinetic energy. It is assumed that no energy production or dissipation takes place in this region.

It is also postulated that the inertial subrange exists when the Reynolds number is high enough to widely separate the energy containing and the dissipation ranges in terms of wave number (i.e. $k_0 >> k_D$), which is always the case for typical jet flow noise problems. Based on this assumption the inertial subrange can cover a wide range of scales, from very small eddies, as small as 60η, to big vortices of order of $L_0/6$. The total noise radiated from the turbulent flow will be strictly dependent to the noise generated from the inertial subrange.

The whole theory about the importance of the inertial subrange in the noise production mechanism can be found in the work of Meechan and Ford (1958) and it will not be completely reproduced here. It is important to know from his work that the frequency sound spectrum scales as:

$$I(x,\omega) \propto x^{-2}\omega^{2-2\alpha} \tag{8}$$

For a five-thirds law turbulence spectrum $\alpha = 5/3$, the sound intensity will be proportional to $\omega^{-4/3}$, but for $\alpha = 5/2$ it turns out to be ω^{-3}. Experimental results for air jets, jet engines, and rockets have shown that the noise spectrum fall off on the high frequency side can scale as ω^{-1} to ω^{-3}, which shows similar range of exponents.

Other authors have devoted special efforts in order to use the energy spectrum associated with the inertial subrange to calculate the emanated noise – Rubinstein and Zhou (1997, 2000), Chen and Kraichnan (1989), Nelkin and Tabor (1990) and Sakar and Hussaini (1993). These works will not be reviewed into this research, since at this point it is important to understand the physical mechanisms behind turbulence and the noise production process. The inertial subrange of the turbulence spectrum is considered, by these theories, the principal contributor to the noise production mechanism.

3.1. Isotropy and Anisotropy

The concepts of turbulence isotropy and anisotropy in a jet flow field are strictly related to the evaluation of the velocity fluctuations, or in other words, to the variations of the Reynolds stresses. Isotropy assumption is that the statistical properties of flow-fluctuations are independent of direction. On the other hand, anisotropy effects are related to local variations of the Reynolds stresses and consequent dependency of direction. This effect is often introduced due to the presence of a mean flow.

The importance of the jet flow anisotropy and its effects on radiated noise have been emphasized by many authors – Ribner (1958), Goldstein and Rosenbaum (1973). Its impact on jet noise predictions, however, has been largely neglected by most engineering models since, at least for round jets; the anisotropy has negligible impact on the shear stress magnitude, which dominates the jet mixing process and therefore the turbulence-related research in this field - Barber (1999).

However, as pointed out by Lilley (1958), the assumption of isotropic turbulence neglects important anisotropic effects such as vorticity stretching. It also neglects the effects of the marked reduction in the lateral integral scale of the turbulence, Townsend (1976). In addition the large scale eddies become mainly long cylindrical structures with a longitudinal scale approximately three times the lateral scale. According to Ribner (1969) the non-isotropic structure of turbulence can have an important effect on the directivity pattern of the noise at sufficiently low frequencies.

Despite the lack of experimental data to account for the real effect of the anisotropy in the jet noise prediction, it is important at least to consider its effects on a jet noise modeling framework. It means that the anisotropy effect could be incorporated in the acoustic model without any need to have a special turbulence modeling for the Reynolds stresses. Renewed interest for including the variations of the normal Reynolds stresses within jet modeling frameworks was prompted by the observation of Khavaran and Krejsa (1998) that including anisotropy effects by modifying RANS-based CFD inputs could help explain observed peak SPL changes with observer angle.

Although this approach may be simplistic from the turbulence standpoint, a general acoustic model taking into account the anisotropy effects may not be considered unwanted. The anisotropy effects in the acoustic modeling can be found in the works of Khavaran and Krejsa (1998), Jordan and Gervais (2003), Almeida (2009) among others.

To account for the effect of anisotropy on aerodynamic mixing noise the usual assumption of isotropic turbulence, is generally replaced with that of an axisymmetric turbulence.

The level of the turbulence anisotropy can be modeled by introducing a ratio of longitudinal to lateral length-scale described by the parameter $\Delta = L_2/L_1$, and a mean square turbulent velocity ratio $\beta = (1-\overline{u_2^2}/\overline{u_1^2})$, were the index 1 refers to the stream-wise direction that is assumed to coincide with the axis of turbulence symmetry. In a span-wise plane, turbulent velocity components for an axisymmetric turbulence are related as:

$$\overline{u_2^2} = \overline{u_3^2} \tag{9}$$

Considering $\beta = (1-\overline{u_2^2}/\overline{u_1^2})$ the turbulence kinetic energy k can be expressed as:

$$k = \frac{1}{2}(\overline{u_1^2} + \overline{u_2^2} + \overline{u_3^2}) = \frac{3}{2}\overline{u_1^2}(1-\frac{2}{3}\beta) \tag{10}$$

The next section will provide some numerical results for single jet flows where these parameters are evaluated in order to check the anisotropy effects in the flowfield. No noise predictions are considered herein.

4. SUBSONIC SINGLE JET FLOWS

A nozzle with D = 50 mm, smooth contraction and sharp lip was used as a test bench for the jet flow noise measurements and aerodynamic numerical simulations – Almeida (2009). A general description of the geometry is depicted in Figure 6. The geometry and experimental data for the numerical model has been collected from the JEAN project (EU Research Programme - FP5) Contract No. G4RD-CT-2000-00313. Experiments for a single flow jet operating at different Mach numbers and temperatures were carried out by Jordan et al. (2002) at the MARTEL facility at CEAT (Centre d'Etudes Aero-dynamiques et Thermiques), Universit de Poitiers. Additional details about the JEAN project and experimental data used in this research can be found in Almeida (2009).

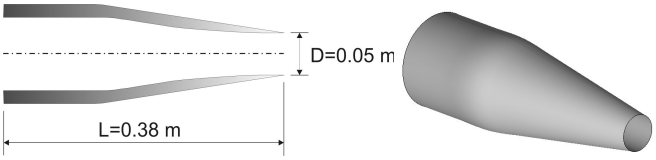

Figure 6. Nozzle geometry for single jet flow.

4.1. Flow Conditions

Table 2 presents the flow conditions for the single jet flows cases investigated. First, an unheated jet is simulated, i.e. the static temperature in the nozzle exit plane, T_j, is equal to the static temperature of the ambient air, T_0.

Table 2. Cases investigated and flow properties

Case	U_j / c_∞	T_j / T_0	U_j (m/s)	c_∞ (m/s)	P_j (Pa)	ρ_∞ (kg/m^3)	P_0 (Pa)	T_0 (K)
1	0.6	1.0	202.65		126900			
2	0.75	1.0	253.31	337.75	144400	1.225	99670	283.15
3	0.9	1.0	303.98		168100			

The length of the computational domain and boundary conditions for the RANS simulations are illustrated in Figure 7. The size of the domain in x and y coordinates was selected after some initial tests in order to check the minimum influence of the downstream and transversal lengths in the flowfield when numerical boundary conditions are applied.

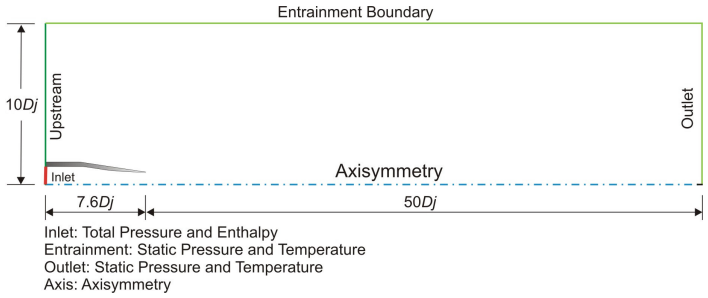

Figure 7. Computational domain and boundary conditions.

The final 2D computational domain discretization consisted of a block structured mesh with 8 blocks and a total of 270000 elements. The mesh points are concentrated to the shear layer region and clustered in the nozzle wall following a 7th-law turbulent boundary layer approach in order to provide a Y^+ close to 30 in this near wall region. A linear growing law is used to increase the elements in axial and radial direction.

Profiles of turbulent kinetic energy, and second-order moments were obtained along two different axial lines, at the centerline and lipline respectively, and at four radial lines according to the Figure 8.

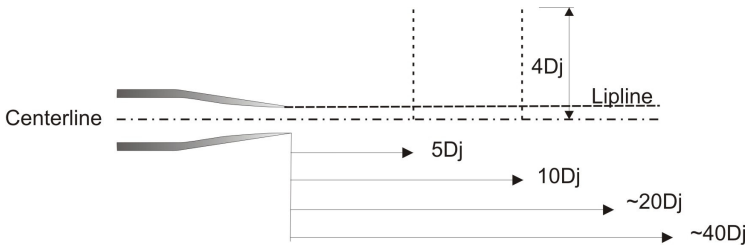

Figure 8. Location of axial and radial profiles – Single jet flow.

5. NUMERICAL RESULTS

The numerical results were obtained through RANS simulations using a Reynolds-Stress Turbulence Model (RSTM). Initially the numerical results for flow dynamics have been compared with experimental data available.

Centerline profiles of u'_{rms} and v'_{rms} are shown in Figure 9 (left and right), respectively. As the potential core was over predicted, the profiles have been normalized with the potential core length, in order to compare the peak values of these quantities. As can be seen, the maximum level is in both cases somewhat under predicted. As mentioned before, the length of the potential core may have influence in the noise prediction. However, more important that matching the potential core length is to predict the right levels of turbulence inside the flow, especially in the shear-layer region. The comparisons with experimental data indicate that a reasonable peak prediction of the turbulence levels are reached.

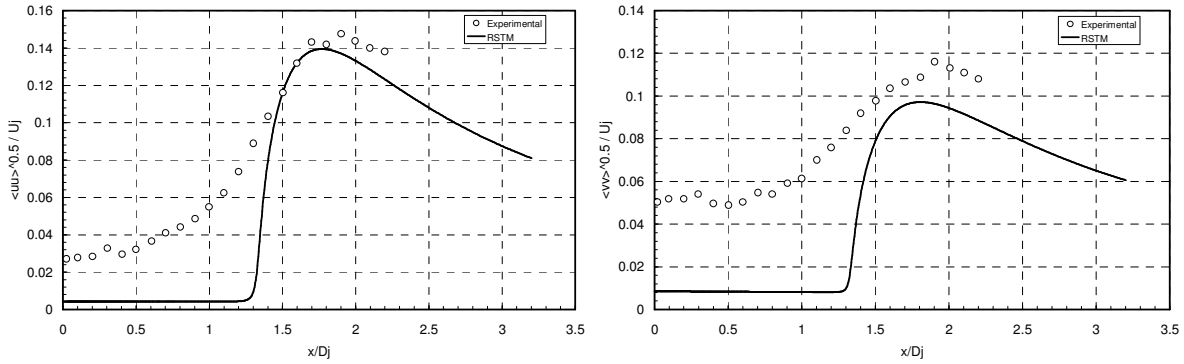

Figure 9. Axial profiles of <uu> and <vv> normalized with potential core length – Mach 0.75.

The next section describes some of the CFD results for different subsonic single jet flows operating at Mach numbers equal to 0.75 and 0.9. For brevity, the results for Mach number 0.6 is not shown in this work.

5.1. Aerodynamic Calculations

Figure 10 shows the contours of the Reynolds stress components $\overline{u'u'}$ and $\overline{v'v'}$ for different Mach numbers of 0.75 and 0.90. The peak values change proportionally for all the cases studied, showing an almost constant ratio of about 0.5 between the longitudinal to lateral stresses. This suggests that the ratio between the longitudinal to lateral scale, as described by the factor $\Delta = L_2 / L_1$ should take values of this order of magnitude.

The relationship between the Reynolds stresses at the nozzle centerline and lipline was calculated and is plotted in Figure 11, including both parameters β and Δ. At this point it is quite interesting to observe that at centreline the relationship between L_2 and L_1 (Δ) is constant throughout the jet domain with a value of 1/3, the same found in some experimental works. However, at the lipline this value is roughly constant and approximately equal to 0.4, which was not found any reference in the literature. Probably due to the fact that sweeping the jet's wake with measurements techniques is quite expensive and time-consuming. Most of the measurements are concentrated in the jet centreline. In addition, it seems that these relationships are a weak function of the Mach number, at least for the cases investigated.

A survey in the literature has been conducted in order to verify some evidence about the relationships $\overline{u_2^2} / \overline{u_1^2}$ and L_2 / L_1 contained in the factors β and Δ respectively. However, no clear evidence on how these factors vary, based on Mach number and temperature, were found. The works of Davies and Fisher (1963) and Grant (1958) suggest that the ratio between the span-wise and stream-wise length scales assumes a value of 1/3. Barber et al. (2001) measured experimentally, for a subsonic cold jet operating a Mach number 0.90, a value of 0.52.

Khavaran and Krejsa (1998) used a value of 0.5 for this ratio without providing additional information about the flowfield. A value of L_2 / L_1 in the range of 0.33 up to 0.5 can be translated to the relationship $\overline{u_2^2} / \overline{u_1^2}$ as a variation in the range of 0.48 up to 0.63, assuming that $L_1 = \left(\overline{u_1^2}\right)^{3/2} / \varepsilon$ and $L_2 = \left(\overline{u_2^2}\right)^{3/2} / \varepsilon$.

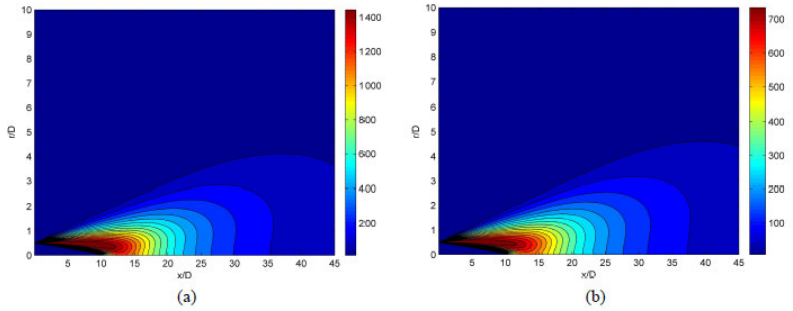

Figure 9. Distribution of Reynolds Stress Tensor components for a Mach 0.75 jet – (a) $\overline{u'u'}$; (b) $\overline{v'v'}$.

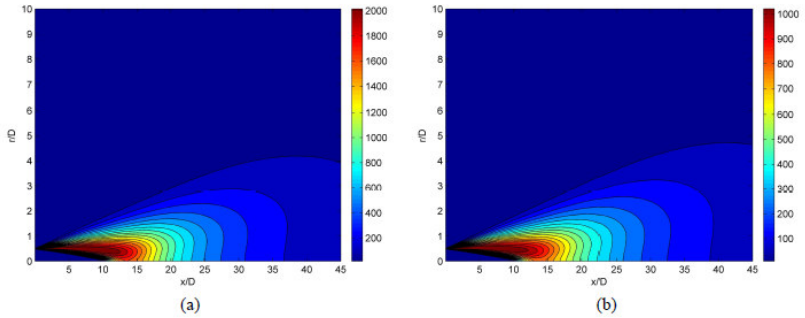

Figure 10. Distribution of Reynolds Stress Tensor components for a Mach 0.90 jet – (a) $\overline{u'u'}$; (b) $\overline{v'v'}$.

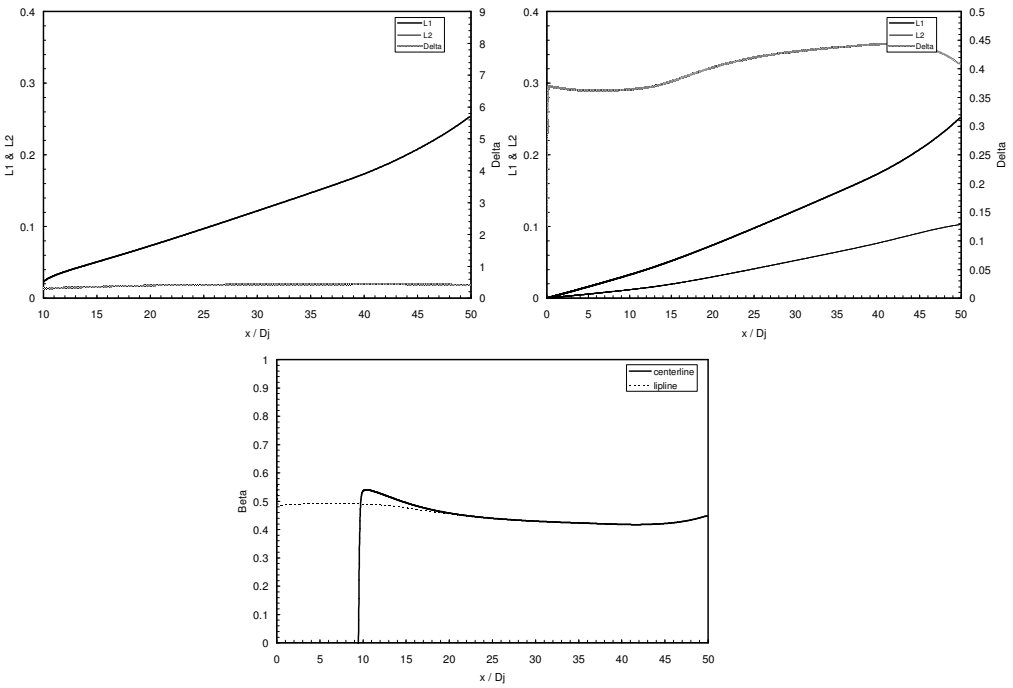

Figure 11. Prediction of the Longitudinal and Transversal length scales - (a) M = 0.75.

6. CONCLUDING REMARKS

The understanding of the noise generation and propagation mechanisms of subsonic jet flows is fundamental for designing the nozzles of turbofan engines aiming at jet noise reduction. A study about the main mechanisms involved in jet noise is being conducted as part of an ongoing research on jet noise carried out at Federal University of Uberlândia – Fluid Mechanics Laboratory (MFlab), also correlating the process of noise generation with the flow turbulence. This work also provided a review of fundamental aspects of fluid dynamics of single flow jets with a long list of references related to the subject. Some numerical simulations performed with a complete Reynolds Stress Modeling (RSTM) turbulence model gave insights about relationship among the transverse and spanwise scales present in the flow field which may have impact on jet noise.

Additional work is required in this field and possibly associated with experimental measurements. One of the possibilities is to include the anisotropy effects in the modeling of the correlation function. More attempts should be put on the understanding and prediction of the large scales noise.

7. REFERENCES

LIGHTHILL, M. J. On sound generated aerodynamically. i - general theory. Proceedings of the Royal Society of London, Series A: Mathematical and Physical Sciences, v. 211, n. 1107, p. 564-587, Mar. 1952.

LIGHTHILL, M. J. On sound generated aerodynamically. II : turbulence as a source of sound. Proceedings of the Royal Society of London, Series A: Mathematical and Physical Sciences, v. 222, n. 1148, p. 1-32, Feb.1954.

MEECHAM, W. C.; FORD, G. W. Acoustic radiation from isotropic turbulence. Journal of Acoustical Society of America, v. 30, p.318-322, 1958.

SILVEIRA-NETO, A. Turbulência nos fluidos aplicada. Uberlândia: Universidade Federal de Uberlândia, 2001. Notas de Aula.

YULE, A. J. Large-scale structure in the mixing layer of a round jet. Journal of Fluid Mechanics, v. 89, pt. 3, p. 413-432, Dec.1978.

TENNEKES, H.; LUMLEY, J. L. A first course in turbulence. Cambridge: MIT Press, 1972.

POPE, S. B. Turbulent flows. Cambridge: Cambridge University Press, 2003.

AZARPEYVAND, M. Some aspects of RANS based jet noise prediction. 2008. 190 f. Thesis (PH.D) - University of Southampton, Southampton.

NASA CENTER. Aeroacoustics of flight vehicles: theory and practice. Washington, DC: NASA 1991. v.1. (NAS 1.61:1258-Vol.-1).

RIBNER, H. S. Quadrupole correlation governing the pattern of jet noise. Journal of Fluid Mechanics, v.38, p.1-24, 1969.

RUBINSTEIN, R.; ZHOU, Y. The frequency spectrum of sound radiated by isotropic turbulence. Physics Letters A, v.267, p.379-383, 2000.

RUBINSTEIN, R.; ZHOU, Y. Time correlation and the frequency spectrum of sound radiated by turbulent flows. Hampton: National Aeronautics and Space Administration, Langley Research Center, 1997. (ICASE report, NAS1-19480)

CHEN, S.Y.; KRAICHNAN, R. H. Sweeping decorrelation in isotropic turbulence. Physics of Fluids A, v.1, n.12, p. 2019-2024, 1989.

NELKIN, M.; TABOR, R. Time correlation and random sweeping in isotropic turbulence. Physics of Fluids A, v.2, p. 81, 1990.

SAKAR, R.; HUSSAINI, M.Y. Computation of the sound generated by isotropic turbulence. Hampton, Va.: National Aeronautics and Space Administration, Langley Research Center, 1993. (ICASE Report 93-74).

RIBNER, H. S. Strength distribution of noise source along a jet. Journal of Acoustical Society of America, v.30, p. 876, 1958.

GOLDSTEIN, M.; ROSENBAUM, B. Effect of anisotropy turbulence on aerodynamic noise. Journal of the Acoustical Society of America, v.54, n.3, p.630-645, 1973.

BARBER, T. J. et al. Assessment of parameters influencing the prediction of shear layer mixing. Journal of Propulsion and Power, v. 15, n. 1, p.45-53, 1999.

LILLEY, G. M. On the noise from air jets. London: H.M.S.O., 1958. (Aeronautical Research Council Report, n. 20376).

TOWNSEND, A. A. The structure of turbulent shear flows. 2 ed. Cambridge: Cambridge University Press, 1976.

KHAVARAN, A.; KREJSA, E. A On the Role of anisotropy in turbulent mixing noise. In.: AIAA/CEAS AEROACOUSTICS CONFERENCE, 4., 1998, Toulouse. Proceedings…Washington, DC: AIAA, 1998. (AIAA Paper N. 98-2289).

JORDAN, P.; GERVAIS, Y. Modelling self and shear noise mechanisms in anisotropy turbulence. In.: AIAA/CEAS AEROACOUSTICS CONFERENCE AND EXHIBIT, 9., 2003, Hilton Head. Proceedings…Washington, DC: AIAA, 2003.(AIAA Paper N. 2003-3318)

ALMEIDA, O., Aeroacoustics of Dual-stream Jets with Application to Turbofan Engines, Instituto Tecnológico da Aeronáutica, Tese de Doutorado, 2009.

JORDAN, P. Results from acoustic field measurements. project deliverable D3.6, JEAN-EU. In.: FRAMEWORK PROGRAM, 5., 2002. Proceedings…Poitiers: Laboratoire d'Etude Aerodynamiques. 2002. G4RD-CT-2000-00313

DAVIES, P. O. A. L.; FISHER, M. J. Statistical properties of the turbulent velocity fluctuations in the mixing region of a round subsonic jet. Southampton: Department of Aeronautics and Astronautics, University of Southampton, 1963. (ISVR Technical Report N. 233).

GRANT, M. L. The large eddies of turbulent motion. Journal of Fluid Mechanics, v. 4, p.149, 1958.

BARBER, T. J.; NEDUNGADI, A., KHAVARAN, A. Predicting the jet noise from high-speed round jets. In.: AIAA AEROSPACE SCIENCES MEETING & EXHIBIT, 39., 2002, Reno. Proceedings…Washington, DC: AIAA, 2001. (AIAA Paper N. 2001-0819).

8. RESPONSIBILITY NOTICE

The author(s) is (are) the only responsible for the printed material included in this paper.